

A DIRECT CONSTRAINT ON THE GAS CONTENT OF A MASSIVE, PASSIVELY EVOLVING ELLIPTICAL GALAXY AT $Z = 1.43^{\S}$

M. T. SARGENT^{1, 2, *}, E. DADDI², F. BOURNAUD², M. ONODERA³, C. FERUGLIO^{4, 5, 6}, M. MARTIG^{7, 8}, R. GOBAT^{2, 9}, H. DANNERBAUER¹⁰, E. SCHINNERER⁷

SUBMITTED TO APJL: *January 31, 2015*

ABSTRACT

In comparison to gas and dust in star-forming galaxies at the peak epoch of galaxy assembly, which are presently the topic of intense study, little is known about the interstellar medium (ISM) of distant, passively evolving galaxies. We report on a deep 3 mm-band search with IRAM/PdBI for molecular gas in a massive ($M_{\star} \sim 6 \times 10^{11} M_{\odot}$) elliptical galaxy at $z = 1.4277$, the first observation of this kind ever attempted. We place a 3σ upper limit of 0.30 Jy km/s on the flux of the $\text{CO}(J=2 \rightarrow 1)$ line or $L'_{\text{CO}} < 8.3 \times 10^9 \text{ K km/s pc}^2$, assuming a line width in accordance with the stellar velocity dispersion of $\sigma_{\star} \sim 330 \text{ km/s}$. This translates to a molecular gas mass of $< 3.6 \times 10^{10} (\alpha_{\text{CO}}/4.4) M_{\odot}$ or a gas fraction of $\lesssim 5\%$ assuming a Salpeter initial mass function (IMF) and an ISM dominated by molecular gas, as observed in local early-type galaxies (ETGs). This low gas fraction approaches that of local ETGs, suggesting that the low star formation activity in massive, high- z passive galaxies reflects a true dearth of gas and a secondary role for inhibitive mechanisms like morphological quenching.

Subject headings: cosmology: observations — galaxies: evolution — galaxies: elliptical and lenticular, cD — galaxies: ISM — ISM: molecules

1. INTRODUCTION

Molecular gas has been detected through rotational CO transitions out to very high redshift, first in highly luminous sources experiencing “bursty” star formation (sub-millimetre galaxies & QSOs; e.g. Greve et al. 2005, Riechers et al. 2006, Maiolino et al. 2007) and subsequently also in galaxies undergoing “main-sequence” (MS) star formation (SF; e.g. Daddi et al. 2008, Tacconi et al. 2010, Geach et al. 2011). Observations show that, when the universe was half its current age, MS galaxies had gas reservoirs approximately 10-fold larger than nearby spiral galaxies (e.g. Daddi et al. 2010a, Tacconi et al. 2013).

It is not known, however, whether the gas content evolves in a synchronised fashion in both active and pas-

sive galaxies, i.e. following a “universal” cosmic decline. Molecular gas is detected in roughly $1/5$ of all local ETGs (this fraction is slightly larger in the field than in clusters; cf. Young et al. 2011) and typically amounts to $\sim 1\%$ of the stellar mass of morphological types E/S0. Do ETG gas fractions increase with redshift? Intuition might expect this as massive high- z ETGs undergo mergers with gas-rich satellites and accrete a fraction of the latter’s gas. Gabor et al. (2010) show that standard quenching mechanisms (gas consumption in mergers, AGN feedback, virial shocks) produce red sequence galaxies with bluer colors than observed at $z = 1-2$ because spheroids in their cosmological hydrodynamic simulations still have substantial residual gas, resulting in excessive SF unless additional quenching mechanisms are invoked. Martig et al. (2009) suggested that fragmentation-prone gas reservoirs can be kept from forming stars when embedded within a stellar spheroid (“morphological quenching”), implying that high- z ETGs could host gas which cannot be tapped to form stars and has thus so far escaped attention. This is also consistent with the long gas consumption time scales Saintonge et al. (2012) find in nearby ETGs.

To obtain a first direct measurement of the currently unknown molecular gas reservoirs of distant passive galaxies we searched for $\text{CO}(J=2 \rightarrow 1)$ line emission from a massive elliptical galaxy at $z \sim 1.5$ with the PdBI. Our target and observations are described in Section 2.2. Results and discussion follow in Sections 3 and 4. We adopt a flat WMAP-7 cosmology ($\Omega_m = 0.273$ and $H_0 = 70.4 \text{ km s}^{-1} \text{ Mpc}^{-1}$; Larson et al. 2011).

2. TARGET DESCRIPTION AND DATA

2.1. *J100239.52+015659.1 - a pBzK-selected, massive, elliptical galaxy at $z = 1.4277$*

A stringent limit on the gas content of distant quiescent galaxies which allows for a meaningful comparison

* E-mail: Mark.Sargent@sussex.ac.uk

¹ Astronomy Centre, Department of Physics and Astronomy, University of Sussex, Brighton, BN1 9QH, UK

² CEA Saclay, DSM/Irfu/Sérvise d’Astrophysique, Orme des Merisiers, F-91191 Gif-sur-Yvette Cedex, France

³ Institut für Astronomie, Departement für Physik, ETH Zürich, Wolfgang-Pauli-Strasse 27, CH-8093 Zürich, Switzerland

⁴ IRAM, 300 rue de la Piscine, F-38406 St. Martin d’Heres, Grenoble, France

⁵ Scuola Normale Superiore, Piazza dei Cavalieri 7, I-56126 Pisa, Italy

⁶ INAF - Osservatorio Astronomico di Roma, via Frascati 33, 00044 Monte Porzio Catone (RM) Italy

⁷ Max-Planck-Institut für Astronomie, Königstuhl 17, D-69117 Heidelberg, Germany

⁸ Centre for Astrophysics & Supercomputing, Swinbourne University, Melbourne, Australia

⁹ KIAS, 85 Hoegiro, Dongdaemun-gu Seoul 130-722, Republic of Korea

¹⁰ Institut für Astronomie, Universität Wien, Türkenschanzstrasse 17, A-1160 Wien, Austria

[§] Based on observations with the Plateau de Bure millimetre Interferometer (PdBI), operated by the Institute for Radio Astronomy in the Millimetre range (IRAM), which is funded by a partnership of INSU/CNRS (France), MPG (Germany) and IGN (Spain).

with nearby ETGs is most readily achieved for high-mass galaxies. We hence selected the most massive galaxy – J100239.52+015659.1 or pBzK-217431 – from the sample of Onodera et al. (2012; “O12” hereafter). pBzK-217431 is a BzK-selected (Daddi et al. 2004), passively evolving, red elliptical galaxy in the COSMOS field with a spectroscopic redshift of $z = 1.4277 \pm 0.0015$ (derived from a high-confidence detection of the 4000 Å break) and an age of ~ 1.6 Gyr (corresponding to the average ‘build’ redshift $z \sim 2.5$ for the bulk of the stars in ETGs in the O12 sample; see Onodera et al. 2015). With a stellar mass¹³ of $6.6^{+0.5}_{-1.9} \times 10^{11} M_{\odot}$ (from SED-fitting in O12) this object is one of the most massive and luminous ($K_{\text{Vega}} = 17.56$) ETGs known at this redshift. It is 5-10 times more massive than star-forming galaxies (SFGs) at a similar redshift followed-up in CO by Daddi et al. (2010a) or the PHIBSS survey (Tacconi et al. 2013). pBzK-217431 lies within 1σ of the local mass-size relation for elliptical galaxies (e.g. Newman et al. 2012) and has an optical surface brightness distribution consistent with the canonical de Vaucouleurs profile (O12, Mancini et al. 2010). Stellar population modelling and SED-fitting indicate that its star formation rate (SFR) is $\lesssim 6 M_{\odot}/\text{yr}$ (Onodera et al. 2015).

2.2. IRAM PdBI 3 mm-band CO($J=2\rightarrow 1$) follow-up

pBzK-217431 was observed in several tracks between June 21-30, 2011 (IRAM project ID *V032*) and May 26-July 19, 2012 (project ID *V09E*), always with five PdBI antennae on-source except for one track in 2012 when only four antennae were available. During both observation campaigns all tracks were carried out in the compact D-configuration (angular resolution: $6.5'' \times 5.7''$), with the 3.6 GHz WideX correlator tuned to the expected frequency of the redshifted CO($J=2\rightarrow 1$) transition at 94.96 GHz ($\nu_{\text{rest}} = 230.538$ GHz). In 2011 the phase centre of the observations lay on pBzK-217431 and in 2012 on a nearby dwarf-like galaxy with photometric redshift $z_{\text{phot}} = 0.215$ (Ilbert et al. 2013), offset $\sim 7''$ from pBzK-217431 (Figure 1c). This shift was applied following the detection of a broad (760 MHz; detected with $S/N = 6.5$ in the uv -plane) emission feature associated with the neighboring galaxy in multiple tracks in 2011. Given the photometric redshift of the dwarf galaxy this could have represented a CO($J=1\rightarrow 0$) line emission feature but the data gathered in 2012 suggested this was an artefact. We reduced the data from the two observing periods individually with the GILDAS software packages CLIC and MAPPING and relying on varying combinations of the calibrators 0851+202, 0906+015, 0923+392, 1005+066, 1040+244, 1055+018, 3C84, 3C273, 3C345, CRL618 and MWC349 for pointing and phase calibration, and on either 0923+392, 1005+066, 3C279, MWC349, 3C84 or 3C345 for flux calibration. Data sets *V032* and *V09E* were subsequently combined after correcting for primary beam attenuation and the phase shift between the two pointing centers. After the flagging of poor visibilities the combined data set has a total 5-antenna (6-antenna) equivalent observing time of 11.59 (7.73) hr and reaches

¹³ In accordance with literature on IMF variations (e.g. Grillo & Gobat 2010, Conroy & van Dokkum 2012, Cappellari et al. 2012) we henceforth adopt a Salpeter (1955) IMF for pBzK-217431 and a Chabrier (2003) IMF for SFGs.

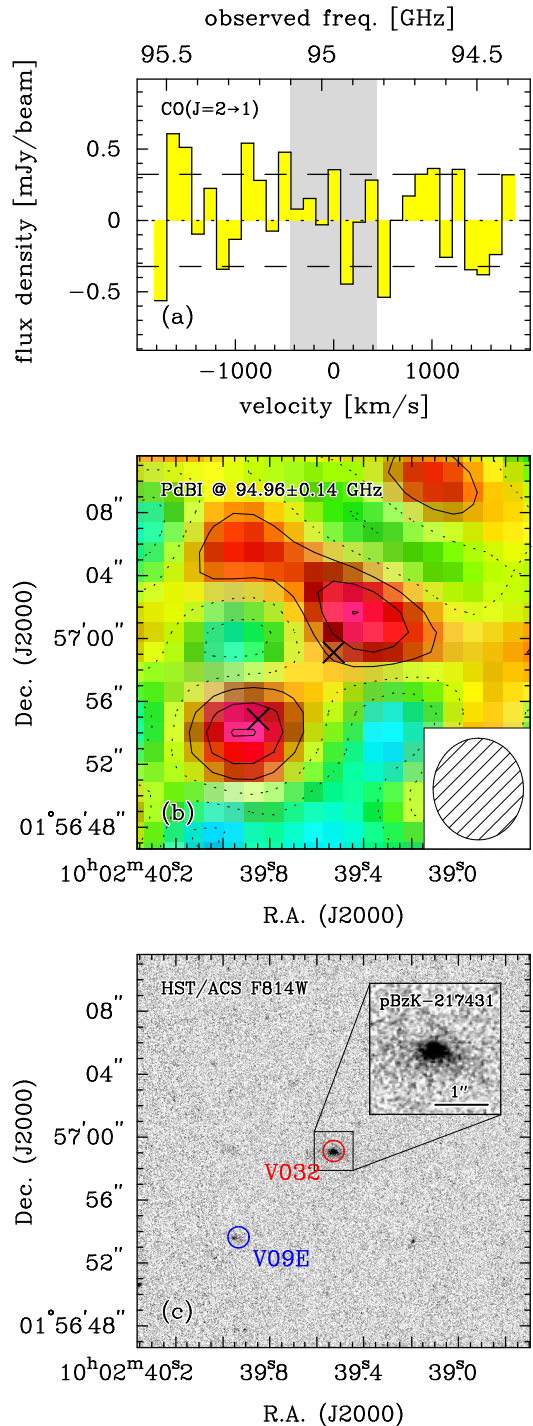


FIG. 1.—: PdBI 3 mm observations of pBzK-217431. (a) Spectrum extracted at the target position within ± 2000 km/s of the expected frequency of redshifted CO($J=2\rightarrow 1$). Dashed lines: $\pm 1\sigma$ noise level for 40 MHz channels. (b) Map of the emission integrated over the expected FWHM of the CO line (280 MHz or 882 km/s; see panel (a), grey area). Solid (dotted) contours: positive (negative) 1 & 2 σ noise level. Inset: synthesized beam. (c) HST *I*-band imaging of pBzK-217431 and surroundings (image size – $30'' \times 30''$; zoom-in size – $2.5'' \times 2.5''$). Blue/red circle: phase centre of the two separate PdBI pointings targeting the pBzK-217431 field (Section 2.2). Pointing centres are indicated with crosses in panel (b).

a noise level of 0.33 mJy/beam in a 40 MHz channel (126 km/s). This sensitivity was not sufficient to detect CO line emission. Figure 1a shows the featureless spectrum binned in 40 MHz channels, extracted at the location of pBzK-217431 and centred on the expected position of redshifted CO($J=2\rightarrow 1$).

3. RESULTS

To set an upper limit on the CO($J=2\rightarrow 1$) line flux we assume that the width of the line is commensurate with the stellar velocity dispersion of pBzK-217431. Since we have no direct measurement of the velocity dispersion we adopt the average¹⁴ $\sigma_* = 330$ km/s of the $1.4 < z < 2.1$ ETG parent sample derived in Onodera et al. (2015). This value agrees well with the velocity dispersions found by other high- z ETG studies (e.g. Newman et al. 2010) and translates to an expected line width (FWHM) of 777 km/s (frequency space: 246 MHz).

Figure 1b shows the flux distribution within $\sim 15''$ of the target position after integration of the 3 mm spectrum over 7 channels (280 MHz) centred on the expected line frequency. While we see a $\sim 3\sigma$ flux concentration $3''$ north of pBzK-217431 in Figure 1b we do not consider this a reliable signature of weak line emission from our target. This is supported by the fact that the total number of $>2\sigma$ pixels in the displayed region is fully consistent with Gaussian statistics. At very low signal-to-noise the most robust estimate of the flux is generally obtained at the phase centre where we detect flux only at 1.2σ significance. The 1σ noise level for the velocity-integrated CO($J=2\rightarrow 1$) line is 0.12 mJy, which allows us to place a 3σ upper limit of $L'_{\text{CO}(J=2\rightarrow 1)} < 8.3 \times 10^9$ K km/s pc² on the line luminosity following Solomon & Vanden Bout (2005; equation 3).

In nearby ETGs atomic hydrogen contributes negligibly to the mass budget (Crocker et al. 2011) so that, assuming this is also true for their high- z counterparts, CO emission is a good proxy for their *entire* gas reservoir. For ATLAS^{3D} ETGs Young et al. (2011) have also shown that CO($J=2\rightarrow 1$) is consistent with thermal excitation and can thus be used as a direct tracer of the molecular gas content. Converting our line flux limit to a constraint on the gas mass of pBzK-217431 requires choosing a CO-to-H₂ conversion factor. ISM conditions in low- z ETGs generally resemble those of local spiral galaxies (dense gas fractions – Krips et al. 2010; H₂ surface densities – Young et al. 2011; dust temperatures – Crocker et al. 2012; low star formation efficiency, SFE – Martig et al. 2013), leading us to adopt a Milky-Way-like $\alpha_{\text{CO}} \sim 4.4 M_{\odot}/(\text{K km/s pc}^2)$. A similar α_{CO} is inferred when considering a metallicity-dependent conversion factor (e.g. Schrubba et al. 2012, Genzel et al. 2012) and using the slightly super-solar, average enrichment $Z/Z_{\odot} \sim 1.2$ of ETGs of the O12 sample. Finally, we note that simulations of high- z elliptical with a range of

¹⁴ A very similar line width is inferred by assuming that velocity dispersion, mass and size are related as $\sigma_*^2 \propto M_*/r_e$ and estimating the velocity dispersion of pBzK-217431 ($M_* = 6.6 \times 10^{11} M_{\odot}$, $r_e = 7.2$ kpc) based on the O12 sample median [σ_* , M_* , r_e] = [330 km/s, $2.2 \times 10^{11} M_{\odot}$, 2.4 kpc]. This re-scaling procedure involving size measurements is only meaningful when all galaxies have similar structural properties; the median Sérsic index and scatter of the O12 sample is 3.2 ± 1.2 , implying that pBzK-217431 lies within 0.5σ of the sample median.

TABLE 1
SOURCE PROPERTIES: pBzK-217431.

quantity/observable	value
R.A. [J2000]	10 ^h 02 ^m 39.527 ^s
Dec. [J2000]	+01 ^d 56 ^m 59.12 ^s
z_{spec}	1.4277 \pm 0.0015
M_* [M_{\odot}]	$6.6^{+0.5}_{-1.9} \times 10^{11}$
r_e [kpc]	7.19 \pm 1.95
Sérsic index n	3.8 \pm 0.6
rms/40 MHz [mJy]	0.33
$I_{\text{CO}(J=2\rightarrow 1)}$ [Jy km/s]	$< 0.30 \sqrt{\left(\frac{\Delta v}{777 \text{ km/s}}\right)}$
$L'_{\text{CO}(J=2\rightarrow 1)}$ [K km/s pc ²]	$< 8.3 \times 10^9$
$M_{\text{mol.}}$ [M_{\odot}]	$< 3.6 \times 10^{10} \left(\frac{\alpha_{\text{CO}}}{4.4}\right)$
f_{gas}	$< 5.1\%$

NOTE. — Properties listed above horizontal divider are from Onodera et al. (2015). Upper limits are quoted at 3σ significance.

gas fractions (~ 10 -50%) and post-processing with Large Velocity Gradient (LVG) models as in Bournaud et al. (2014) predict α_{CO} -values comparable to that of the Milky Way as well.

Our observations hence constrain the gas mass of pBzK-217431 to be $M_{\text{gas}} < 3.6 \times 10^{10} (\alpha_{\text{CO}}/4.4) M_{\odot}$. This is similar in magnitude to gas masses found in MS galaxies at $1 < z < 2$, whereas pBzK-217431 is an order of magnitude more massive, resulting in a 3σ upper limit of $f_{\text{gas}} = M_{\text{gas}}/(M_* + M_{\text{gas}}) < 5.1\%$ on its gas fraction¹⁵. This is a factor of 10 lower than in most known MS galaxies with CO-detections at the peak epoch of galaxy formation. The properties of pBzK-217431 are summarized in Table 1.

4. DISCUSSION

4.1. The gas content of pBzK-217431 in the galaxy evolution context

As a proxy for the redshift evolution of ETG gas fractions which involves no assumptions about α_{CO} we compare in Figure 2a the L'_{CO}/M_* ratio of pBzK-217431 with sample averages for MS galaxies at $z < 2.5$ and $z \sim 0$ ETGs¹⁶ from ATLAS^{3D} (Young et al. 2011). Median L'_{CO}/M_* values of literature MS galaxy samples are plotted with spiral galaxy symbols: $z \sim 0$ – HERACLES & COLD GASS (Leroy et al. 2009, Saintonge et al. 2011); $0.1 < z < 0.6$ – Daddi et al. (2010b), Geach et al. (2011) & EGN0G (Bauermeister et al. 2013); $1.1 < z < 1.7$ & $z > 2$ – Daddi et al. (2010a) & PHIBSS (Tacconi et al. 2013). The continuous evolution of the gas content in $z < 2.5$ MS galaxies with $M_* \sim 5 \times 10^{10} M_{\odot}$, the typical mass of all these samples, is traced by the grey band, based on the scaling relations between M_* , SFR, molecular gas mass $M_{\text{mol.}}$ and α_{CO} calibrated in Sargent et al.

¹⁵ Although M_{gas} appears in both numerator and denominator of the expression for f_{gas} , it is nevertheless possible to define a meaningful upper limit on the gas fraction as the inverse $1/f_{\text{gas}} = 1 + M_*/M_{\text{gas}}$ represents a well defined *lower* limit on $1/f_{\text{gas}}$ when, as here, only an upper limit on M_{gas} is available.

¹⁶ Masses for ATLAS^{3D} ETGs are the product of the r -band luminosity and mass-to-light ratios from JAM modelling in Cappellari et al. (2012).

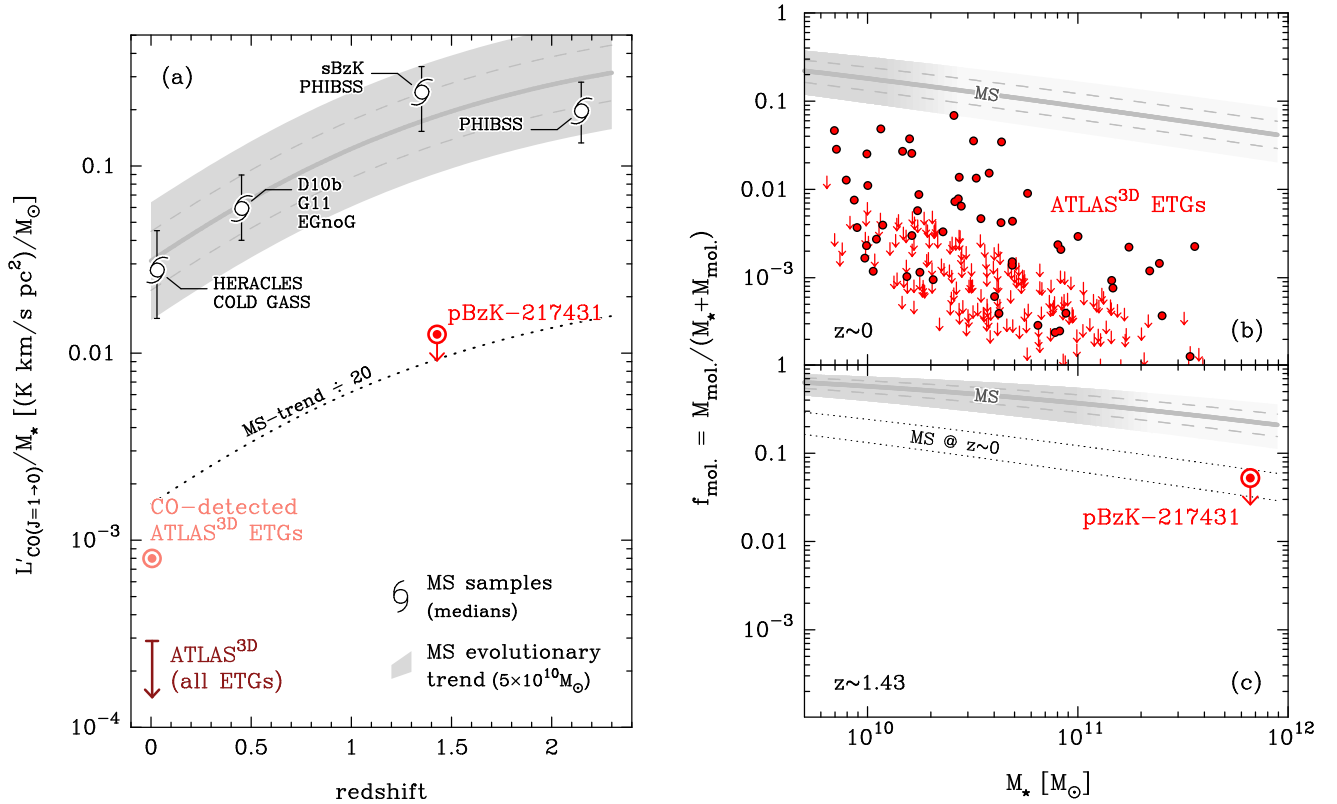


FIG. 2.— CO emission and gas content of pBzK-217431 compared to ATLAS^{3D} ETGs and $0 < z < 2.5$ main-sequence (MS) galaxies. (a) 3σ upper limit on the ratio of CO luminosity and stellar mass M_* for pBzK-217431, plus typical L'_{CO}/M_* ratios measured for ATLAS^{3D} ETGs (light red – median of CO-detected ETGs; dark red – upper limit on sample median for *all* ATLAS^{3D} ETGs) and literature MS galaxy samples. (See annotations for survey names. Author abbreviations: D10b – Daddi et al. 2010b; G11 – Geach et al. 2011). For MS galaxies we plot the median L'_{CO}/M_* and redshift of the combined samples; error bars illustrate the 1σ scatter in the data. Dark grey, solid line: expected redshift evolution of L'_{CO}/M_* for an average MS galaxy with $M_* = 5 \times 10^{10} M_\odot$ (Section 4.1). Dashed lines (edges of light grey shading): L'_{CO}/M_* ratio for $\pm 1\sigma$ ($\pm 2\sigma$) outliers to the MS.

(b) Molecular gas fraction f_{mol} for ATLAS^{3D} ETGs compared to the average relation between gas fraction and M_* for massive $z \sim 0$ MS galaxies. (Shading/lines as in panel (a); in panels (b) and (c) the grey shading fades away at the cross-over mass, above which ETGs dominate SFGs by number at the respective redshift.)

(c) As in panel (b) but highlighting the paucity of gas in pBzK-217431 with respect to typical gas fractions of massive MS galaxies at the same redshift. Dotted lines: $\pm 1\sigma$ scatter of f_{mol} in $z \sim 0$ MS galaxies (cf. panel (b)).

(2014). For ATLAS^{3D} ETGs we plot the median of the subset of CO-detected ETGs (22% of ATLAS^{3D} ETGs) and an upper limit on the median L'_{CO}/M_* ratio of the overall sample, placed at the 84th percentile of the Kaplan & Meier (1958) distribution which accounts for both the CO-detections and non-detections. The upper limit on the CO-deficit of pBzK-217431 relative to $z \sim 1.4$ MS galaxies is ~ 20 (see Figure 2a), comparable to that of CO-detected ATLAS^{3D} ETGs relative to local spirals. This limit is not stringent enough for a helpful comparison with the full ATLAS^{3D} ETG sample median.

In the introduction we posed the question whether gas fractions in star-forming and quiescent galaxies evolved with time by equal proportions. A quantitative comparison must involve the fact that pBzK-217431 is about $10\times$ as massive as ATLAS^{3D} ETGs on average. Figures 2b/c show that gas fractions of local ETGs decrease with M_* down to $\lesssim 1\%$ at the highest masses. Our observations are not sufficiently deep to start testing whether, at fixed M_* , f_{gas} for quiescent galaxies is constant over the last

~ 10 Gyr. Over this period gas fractions of normal galaxies with masses at or above the knee of the stellar mass function ($M^* \sim 10^{11} M_\odot$) evolve by a factor 4-5 (from a few to about 15-30%; cf. Figure 2b/c or Tacconi et al. 2013, Scoville et al. 2014). For pBzK-217431 and local ETGs the values are $< 5\%$ and $< 1\%$, resp., such that we cannot exclude a similar ~ 5 -fold evolution of f_{gas} for ETGs based solely on our observations.

Combining our upper limit on the gas mass of pBzK-217431 with SFR-estimates from ETG stacked optical spectra and optical-to-IR SEDs in Onodera et al. (2015) and Man et al. (2014), we can get a rough idea of its SFE. The average specific SFR (sSFR) of $< 10^{-11} \text{ yr}^{-1}$ for the ETG sample of O12 is consistent with the upper limit found for the *dust-obscured* SFR in the largest mass bin of a larger sample of photometrically selected quiescent galaxies in Man et al. (2014). Applied to pBzK-217431 this level implies a SFR of $< 5\text{-}10 M_\odot/\text{yr}$, while SED fitting performed by Man et al. (2014) suggests SFR $\sim 0.4 M_\odot/\text{yr}$. The resulting, loose constraint on the

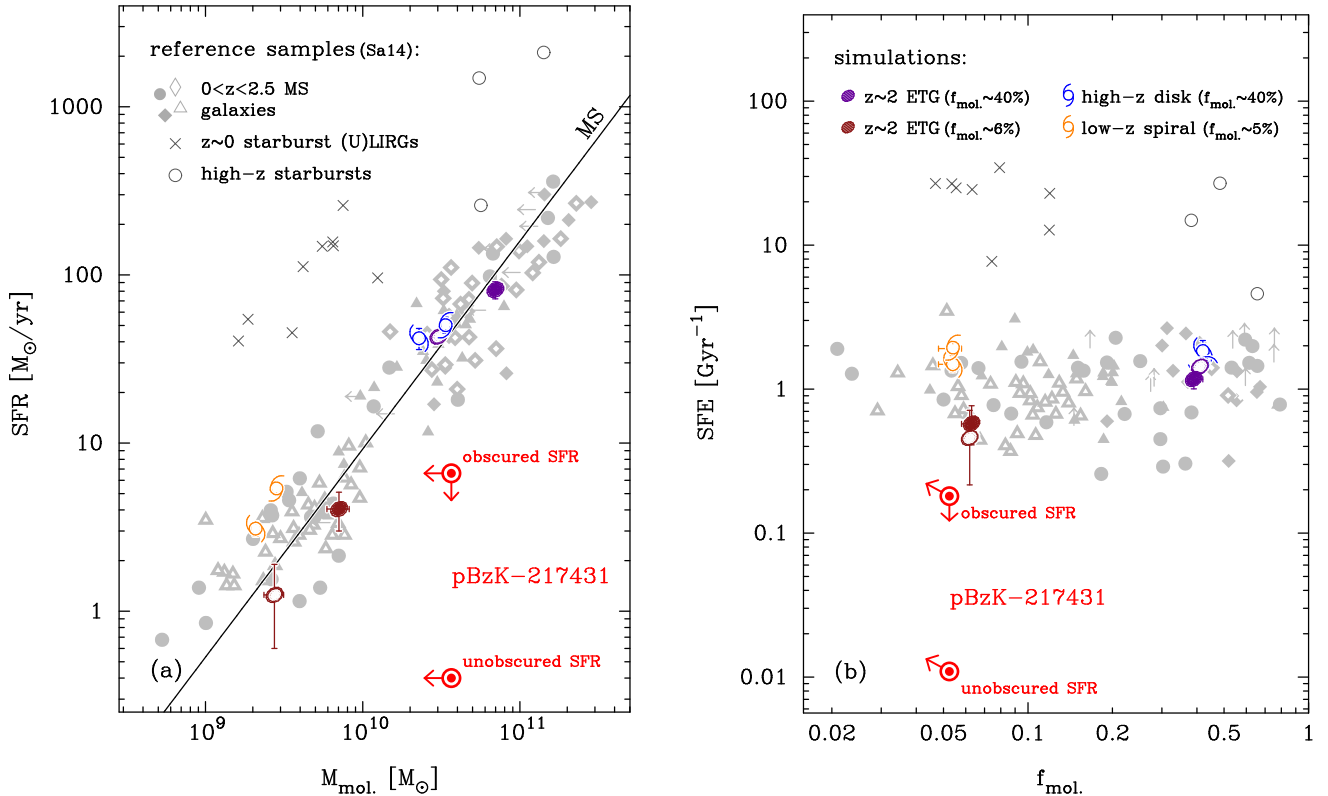


FIG. 3.— Location of pBzK-217431 in the integrated Schmidt-Kennicutt diagramme (a) and in SFE vs. $f_{\text{mol.}}$ space (b). Data points scattering around the ‘MS’ SF law in panel (a) are literature main-sequence galaxies (compiled in Sargent et al. 2014; Sa14). Crosses (open circles): low- (high-) z starbursts with measured α_{CO} and typically $\sim 15\times$ higher SFE than MS galaxies. Indicative SFR estimates for pBzK-217431 are from average spectral/SED properties of $z \sim 1.5$ ETG samples (O12, Man et al. 2014). Colored symbols indicate the properties of simulated gas-rich/gas-poor (purple/dark red) ETGs and gas-rich/gas-poor (blue/orange) disks (see discussion in text). Error bars on simulated data points illustrate variations in the simulations of these quantities over a few 100 Myr.

gas depletion time $\tau_{\text{depl.}} = M_{\text{gas}}/\text{SFR}$ is < 90 ($\alpha_{\text{CO}}/4.4$) Gyr (see Figure 3). Presuming that, similar to nearby ETGs (e.g. Saintonge et al. 2012; Martig et al. 2013), high- z ETGs have 2-5 \times lower SFEs than disk galaxies this means that a roughly 10-fold sensitivity increase compared to our PdBI observations would be required to detect an expected gas reservoir of order $10^9 M_{\odot}$. This highlights the need for alternative ISM tracers or deeper observations, e.g. with ALMA, in order to advance our knowledge of the cold gas in distant quiescent galaxies.

4.2. Considerations on feedback and quenching

Galaxies as massive as pBzK-217431 at $z = 1.4277$ are prime candidates for suffering so-called ‘mass quenching’ (e.g. Peng et al. 2010; Figure 15). Various different mechanisms potentially contribute to mass quenching, and more widespread observations of the ISM of quenched galaxies as presented here should ultimately reveal which (combination) of these is most important. Examples of internal processes are gravitational/morphological quenching (Martig et al. 2009, Genzel et al. 2014), AGN-feedback (e.g. Granato et al. 2004) or SF-activity (e.g. Ceverino & Klypin 2009). Feedback suppresses SF by removing gas, while simulations of morphological quenching have shown that the SFR of ETGs can remain minimal for several Gyr, notwithstanding gas fractions of 5-10% (cf. Figure 3

in Martig et al. 2009). Our non-detection for pBzK-217431 thus indicates that massive high- z ellipticals at high redshift are truly gas-poor. We illustrate this with Figure 3b which compares sSFR(s) and molecular gas fraction(s) for pBzK-217431 and low- and high- z MS galaxies with simulated $z \sim 2$ ETGs (purple – simulated ETG with $f_{\text{mol.}} \sim 50\%$; dark red – simulated $f_{\text{mol.}} \lesssim 10\%$) having $M_{\star} \sim 4 \times 10^{10}$ (open symbols) and $\sim 10^{11} M_{\odot}$ (filled symbols). These simulations include those from Bournaud et al. (2014) and similar models with other parameters (galaxy type and gas fraction) with 3 pc resolution. They are idealized closed-box models with a chosen initial stellar structure and gas fraction, evolved for a few dynamical times including self-gravity, hydrodynamics, cooling and stellar feedback to compute the phase-space distribution of the ISM and the associated SFE. In gas-rich simulated ETGs, morphological quenching is ineffective, as evidenced by the fact that these systems have the same SFEs as both observed and simulated gas-rich disk galaxies. Conversely, morphological quenching could be responsible for the small (comparable to the dispersion of the SF-law) SFE-offset between the gas-poor simulated ETGs and simulated $z \sim 0$ disks (orange spirals). The low SFRs of massive, high- z ellipticals are thus not the result of unusually low SFE caused by gravitational stabilization of gas reservoirs, but morphological quenching might shut down SF com-

pletely in already gas-poor ETGs. Note that the absence of gas need not be the outcome of active expulsion by AGN or stellar feedback. Sub-millimeter galaxies as the commonly assumed progenitors of early ellipticals usually have sufficiently short gas consumption times (e.g. Bothwell et al. 2013) for reservoir-depletion to well below the sensitivity of our observations of pBzK-217431.

5. SUMMARY

We presented the outcome of a deep IRAM/PdBI 3mm search for CO($J=2\rightarrow 1$) emission from pBzK-217431, a massive, passively evolving elliptical galaxy at $z=1.4277$. Though undetected in CO, we could infer a 3σ upper limit of 5.1% for its gas fraction. This is almost $10\times$ below the typical f_{gas} of MS galaxies at the same epoch and comes close to the gas fractions of local ATLAS^{3D} ETGs, although our limit is not stringent enough for a direct comparison with the most massive ellipticals in the nearby universe where $f_{\text{gas}} \sim 1\%$. Ob-

servational data on the gas content of quiescent galaxies not only tells us about the currently unknown contribution of such galaxies to the cold gas history of the Universe (e.g. Walter et al. 2014, Sargent et al. 2015), it also provides insight into how/which quenching and feedback processes influence the ISM of the host galaxy (e.g. Ciotti & Ostriker 1997). Our gas fraction measurement for pBzK-217431 leads us to speculate that moderate-sized, gravitationally stabilized gas reservoirs are not widespread among massive high- z ellipticals and that their low SFR reflects a paucity of gas, caused by either feedback or exhaustion of their gas reservoir by prior SF activity.

We thank J. M. Winters, A. Cibinel, P.-A. Duc and M. Krips for helpful suggestions and/or data reduction support. MTS, ED, RG & HD acknowledge funding from ERC-StG #240039 and grant ANR-08-JCJC-0008, FB funding from ERC-StG #257720.

REFERENCES

- Bauermeister, A., Blitz, L., Bolatto, A., et al. 2013, *ApJ*, 768, 132
 Bothwell, M. S., Aguirre, J. E., Chapman, S. C., et al. 2013, *ApJ*, 779, 67
 Bournaud, F., Daddi, E., Weiss, A., et al. 2014, arXiv:1409.8157
 Cappellari, M., McDermid, R. M., Alatalo, K., et al. 2012, *Nature*, 484, 485
 Ceverino, D., & Klypin, A. 2009, *ApJ*, 695, 292
 Chabrier, G. 2003, *PASP*, 115, 763
 Ciotti, L., & Ostriker, J. P. 1997, *ApJ*, 487, L105
 Conroy, C., & van Dokkum, P. G. 2012, *ApJ*, 760, 71
 Crocker, A. F., Bureau, M., Young, L. M., & Combes, F. 2011, *MNRAS*, 410, 1197
 Crocker, A., Krips, M., Bureau, M., et al. 2012, *MNRAS*, 421, 1298
 Daddi, E., Cimatti, A., Renzini, A., et al. 2004, *ApJ*, 617, 746
 Daddi, E., Dannerbauer, H., Elbaz, D., et al. 2008, *ApJ*, 673, L2
 Daddi, E., Bournaud, F., Walter, F., et al. 2010, *ApJ*, 713, 686
 Daddi, E., Elbaz, D., Walter, F., et al. 2010, *ApJ*, 714, L118
 Gabor, J. M., Davé, R., Finlator, K., & Oppenheimer, B. D. 2010, *MNRAS*, 407, 749
 Geach, J. E., Smail, I., Moran, S. M., et al. 2011, *ApJ*, 730, L19
 Genzel, R., Tacconi, L. J., Combes, F., et al. 2012, *ApJ*, 746, 69
 Genzel, R., Förster Schreiber, N. M., Lang, P., et al. 2014, *ApJ*, 785, 75
 Granato, G. L., De Zotti, G., Silva, L., Bressan, A., & Danese, L. 2004, *ApJ*, 600, 580
 Greve, T. R., Bertoldi, F., Smail, I., et al. 2005, *MNRAS*, 359, 1165
 Grillo, C., & Gobat, R. 2010, *MNRAS*, 402, L67
 Ilbert, O., McCracken, H. J., Le Fèvre, O., et al. 2013, *A&A*, 556, AA55
 Kaplan, E. L. & Meier, P. 1958, *J. Am. Statist. Assoc.*, 53, 457
 Krips, M., Crocker, A. F., Bureau, M., Combes, F., & Young, L. M. 2010, *MNRAS*, 407, 2261
 Larson, D., Dunkley, J., Hinshaw, G., et al. 2011, *ApJS*, 192, 16
 Leroy, A. K., Walter, F., Bigiel, F., et al. 2009, *AJ*, 137, 4670
 Maiolino, R., Neri, R., Beelen, A., et al. 2007, *A&A*, 472, L33
 Man, A. W. S., Greve, T. R., Toft, S., et al. 2014, arXiv:1411.2870
 Mancini, C., Daddi, E., Renzini, A., et al. 2010, *MNRAS*, 401, 933
 Martig, M., Bournaud, F., Teyssier, R., & Dekel, A. 2009, *ApJ*, 707, 250
 Martig, M., Crocker, A. F., Bournaud, F., et al. 2013, *MNRAS*, 432, 1914
 Muzzin, A., Marchesini, D., Stefanon, M., et al. 2013, *ApJ*, 777, 18
 Newman, A. B., Ellis, R. S., Treu, T., & Bundy, K. 2010, *ApJ*, 717, L103
 Newman, A. B., Ellis, R. S., Bundy, K., & Treu, T. 2012, *ApJ*, 746, 162
 Onodera, M., Renzini, A., Carollo, M., et al. 2012, *ApJ*, 755, 26 (O12)
 Onodera, M., Carollo, C. M., Renzini, A., et al. 2015, arXiv:1411.5023
 Peng, Y.-J., Lilly, S. J., Kovač, K., et al. 2010, *ApJ*, 721, 193
 Riechers, D. A., Walter, F., Carilli, C. L., et al. 2006, *ApJ*, 650, 604
 Saintonge, A., Kauffmann, G., Kramer, C., et al. 2011, *MNRAS*, 415, 32
 Saintonge, A., Tacconi, L. J., Fabello, S., et al. 2012, *ApJ*, 758, 73
 Salpeter, E. E. 1955, *ApJ*, 121, 161
 Sargent, M. T., Daddi, E., Béthermin, M., et al. 2014, *ApJ*, 793, 19
 Sargent, M. T., Daddi, E., et al. 2015, *ApJ*, in prep.
 Schrubba, A., Leroy, A. K., Walter, F., et al. 2012, *AJ*, 143, 138
 Scoville, N., Aussel, H., Sheth, K., et al. 2014, *ApJ*, 783, 84
 Solomon, P. M., & Vanden Bout, P. A. 2005, *ARA&A*, 43, 677
 Tacconi, L. J., Genzel, R., Neri, R., et al. 2010, *Nature*, 463, 781
 Tacconi, L. J., Neri, R., Genzel, R., et al. 2013, *ApJ*, 768, 74
 Walter, F., Decarli, R., Sargent, M., et al. 2014, *ApJ*, 782, 79
 Young, L. M., Bureau, M., Davis, T. A., et al. 2011, *MNRAS*, 414, 940